mathematics

MDPI

Article

Multiscale Kinetic Model for Immune Reaction in Coeliac Disease

Diletta Burini [1], Damian A. Knopoff [2,*] and Lidia Serrano [2]

[1] Department of Mathematics and Computer Sciences, University of Perugia, Via Vanvitelli, 1, 06123 Perugia, Italy; diletta.burini@unipg.it
[2] Faculty of Engineering, University of Deusto, Avda. Universidades, 24, 48007 Bilbao, Spain; lidia.serrano@deusto.es
* Correspondence: d.knopoff@deusto.es

Abstract

This paper presents a multiscale model that captures the complex dynamics of coeliac disease, a chronic T-cell-mediated autoimmune disorder triggered by gluten ingestion in genetically susceptible individuals. Grounded in the mathematical kinetic theory of active particles, the model captures the intricate dynamics of the immunological cascade that leads to small intestinal damage, involving complex interactions across molecular, cellular, and tissue scales. This approach explicitly models the different functional subsystems involved and examines the role of molecular messengers in shaping these dynamics, focusing on gluten recognition and immune system activation. Simulations demonstrate that the model can reproduce significant clinical and biological observations of coeliac disease, suggesting its potential to inform therapeutic strategies.

Keywords: coeliac disease; mathematical modeling; kinetic theory; immune competition

MSC: 92C60; 92D30

1. Introduction

According to the European Society for Pediatric Gastroenterology, Hepatology, and Nutrition (ESPGHAN) guidelines, coeliac disease (CD) is defined as a systemic immune-mediated disorder triggered by gluten in genetically susceptible individuals [1]. It is characterised by a variable combination of clinical manifestations, disease-specific antibodies, HLA-DQ2 or HLA-DQ8 haplotypes, and enteropathy. The disease is associated with intestinal damage, including increased numbers of intraepithelial and lamina propria lymphocytes, villous atrophy, mucosal remodelling, and the presence of anti-tissue transglutaminase (anti-TG2) antibodies [2].

Until relatively recently, CD was previously considered primarily a malabsorption syndrome triggered by gluten rather than a complex immune-mediated disorder. However, advances in research have substantially improved the understanding of its pathophysiology [3,4], allowing the identification of clinical conditions previously attributed to other diagnoses. As a result, the number of diagnosed cases has increased markedly, and CD has become a significant public health concern in many countries. A systematic review and meta-analysis published in 2018 reported a global seroprevalence of 1.4% and a biopsy-confirmed prevalence of 0.7% [5].

Academic Editor: Guowei Wei

Received: 5 March 2026
Revised: 31 March 2026
Accepted: 11 April 2026
Published: 16 April 2026

Although diagnostic rates and scientific knowledge have grown considerably in recent years, research on CD remains in an active phase of development, highlighting the need for disease-specific mathematical models to improve understanding of its mechanisms [6].

At present, the only effective treatment for CD is a strict, lifelong gluten-free diet. The development of alternative therapeutic strategies relies on a detailed understanding of the mechanisms involved in disease onset and progression, including altered intestinal permeability and autoimmune responses.

In individuals with coeliac disease (CD), gluten ingestion results in the generation of peptides that persist within the intestinal lumen due to incomplete proteolytic digestion. These peptides can cross the epithelial barrier and reach the lamina propria. Tissue transglutaminase 2 (TG2), released from damaged enterocytes or present extracellularly, deamidates specific glutamine residues within gluten peptides, converting them into negatively charged glutamate residues [7]. This modification increases the binding affinity of gluten-derived peptides to HLA-DQ2 and HLA-DQ8 molecules expressed on antigen-presenting cells in genetically susceptible individuals [8]. The resulting peptide–HLA complexes are recognised by gluten-specific $CD4^+$ T lymphocytes located predominantly in the lamina propria, leading to activation of the adaptive immune response, B-cell stimulation, and production of anti-TG2 antibodies. Activated $CD4^+$ T-cells secrete pro-inflammatory cytokines such as IFN-γ, thereby amplifying mucosal inflammation. This inflammatory milieu promotes the activation of cytotoxic $CD8+$ intraepithelial lymphocytes (IELs), which mediate epithelial cell damage and contribute to villous atrophy, a hallmark feature of the disease [9]. Recent studies have shown that the activation of cytotoxic IELs and the resulting epithelial damage require cooperation between cytokines released by gluten-specific $CD4^+$ T-cells [10]. Activation of IELs enhances the production of IFN-γ and cytotoxic molecules and upregulates the expression of natural killer receptors [11]. A more detailed discussion of these mechanisms can be found in the doctoral thesis of Martínez [2].

Mathematical modelling of coeliac disease has evolved substantially over the past decades, reflecting a broader shift toward quantitative and systems-level approaches in immunology and gastroenterology. Early contributions relied on phenomenological or statistical descriptions of clinical manifestations, such as growth impairment and recovery under a gluten-free diet [12]. More recent work has introduced mechanistic frameworks grounded in systems biology, aiming to capture the interplay between gluten exposure, epithelial barrier regulation [13], and the adaptive immune response, including the role of HLA-DQ2/8 complexes [14]. These developments highlight the inherently multiscale nature of coeliac disease, where processes ranging from peptide processing and zonulin-mediated permeability changes to T-cell activation and cytokine-driven tissue damage interact across molecular, cellular, and tissue levels [15].

Within this context, kinetic and agent-based approaches—particularly those inspired by the kinetic theory of active particles (KTAP)—have emerged as powerful tools for describing interacting biological populations whose behaviour depends on internal states, external cues, and adaptive responses [16,17]. KTAP-based models have been successfully applied to immune competition, signalling dynamics, and host–pathogen interactions [18], and provide a natural foundation for studying the coupling between gluten translocation, epithelial permeability, and immune activation in coeliac disease. In this article, we extend the KTAP framework to derive a genuinely multiscale model that integrates gluten dynamics, zonulin-mediated permeability modulation, T-cell activation, and cytokine production, incorporating molecular messengers [19–21]. This perspective aligns with the growing recognition—reinforced by the 2025 Nobel Prize in Medicine [22]—that immune phenomena must be understood through the coordinated action of processes operating across multiple organisational scales.

The paper is structured as follows: Section 2 introduces the mathematical structure, presents the mathematical model, and analyses the main analytical properties of the resulting integro-differential system. Section 3 explores its qualitative behaviour through numerical simulations, including single gluten exposure, repeated dietary intake, and variations in immune proliferation rates. Finally, Section 4 discusses the implications of the results and outlines perspectives for future research.

2. A Multiscale KTAP Model for Gluten–Immune Interactions in Coeliac Disease

In this section, we formulate a multiscale mathematical model for the interaction between dietary gluten and the immune system in coeliac disease, within the framework of the KTAP. This approach is designed to describe systems of interacting living entities characterised by heterogeneity, nonlinear interactions, and feedback mechanisms, which cannot be adequately captured by classical compartmental models [17].

The KTAP framework provides a suitable theoretical foundation for describing systems of interacting living entities, referred to as *active particles* (a-particles). These particles are grouped into aggregations in which each entity expresses the same biological function, encoded by an internal variable called *activity*. Such aggregations are referred to as *functional subsystems* (FSs).

The microscopic state of the system is described by a family of distribution functions

$$f_i = f_i(t,u) : \ [0,T] \times D_u \to \mathbb{R}_+, \quad i = 1, \dots, n$$

where $u \in D_u$ denotes the activity variable and the index i identifies the i-th FS.

Macroscopic variables of biological relevance are obtained as weighted moments of the distribution functions. In particular, the density of each FS is defined as

$$n_i = n_i(t) = \int_{D_u} f_i(t,u)\, du,$$

while the mean activity is given by

$$a_i = a_i(t) = \frac{1}{n_i(t)} \int_{D_u} u\, f_i(t,u)\, du.$$

According to the KTAP approach, the time evolution of a general system composed of n FSs is governed by a system of balance equations of the form

$$\partial_t f_i(t,u) = J_i[\mathbf{f}](t,u) = \left(\mathcal{G}_i - \mathcal{L}_i + \mathcal{P}_i - \mathcal{D}_i\right)[\mathbf{f}](t,u), \tag{1}$$

where $\mathbf{f} = \{f_i\}$ denotes the collection of all distribution functions. The operator J_i models gain and loss mechanisms in the elementary volume $[u, u+du]$ of the activity space. Specifically, $\mathcal{G}_i$ and $\mathcal{L}_i$ describe conservative interactions, while $\mathcal{P}_i$ and $\mathcal{D}_i$ account for proliferative and destructive processes, respectively [19].

For FSs that do not exhibit an internal activity structure, the description naturally reduces to scalar densities concentrated at a fixed activity value.

In the context of coeliac disease, the proposed framework explicitly accounts for dietary gluten peptides, immune cell populations with heterogeneous activation states, molecular messengers mediating immune responses, and a macroscopic variable representing intestinal permeability. The coupling between microscopic kinetic dynamics and macroscopic tissue properties gives rise to nonlinear feedback loops that are known to be central to the onset and persistence of the disease.

The following subsections introduce the specific FSs considered in the model, the associated kinetic equations, and the biological interpretation of the interaction mechanisms encoded in the mathematical structure.

2.1. Functional Subsystems and Scales

We consider five FSs, together with one macroscopic tissue variable representing intestinal permeability. A schematic representation of the FSs and interactions is presented in Figure 1. From a physiological point of view, Figure 2 illustrates the pathway encoded in the KTAP model: it links the translocation of dietary gluten peptides across the epithelium with zonulin-mediated modulation of permeability, the activation of gluten-specific T-cells, and the subsequent secretion of effector cytokines. The functional subsystems f_1 to f_5 formalize these coupled processes across molecular, cellular, and tissue scales, while the feedback loops between permeability and gluten transfer capture the amplification mechanisms characteristic of the coeliac condition. As in the KTAP framework, each FS is described by a distribution function over a microscopic activity variable, whenever appropriate.

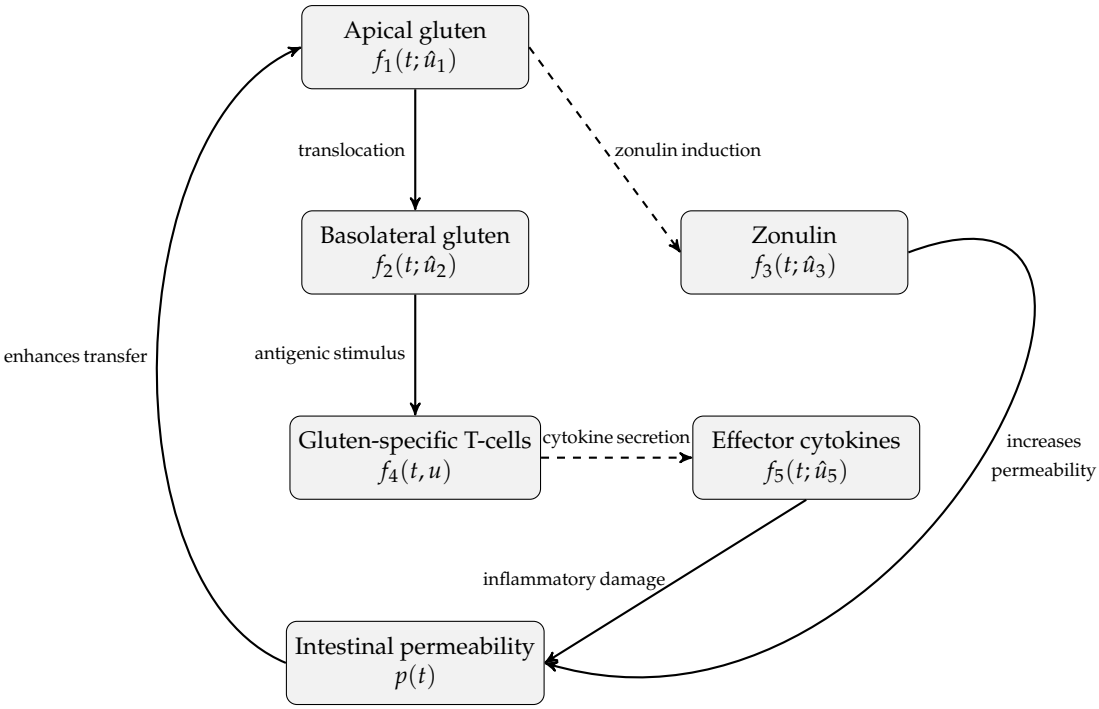

Figure 1. Schematic representation of the multiscale interactions in the KTAP model for coeliac disease.

FS1 ($i = 1$): Apical gluten. This subsystem models the dynamics of immunogenic gluten peptides (e.g., gliadin-derived fragments) present in the intestinal lumen at the apical surface of the small intestine. Since we do not attribute an internal activity state to these peptides, the FS is described by a scalar density

$$f_1 = f_1(t;\hat{u}_1),$$

which may be interpreted as the concentration of gluten peptides in the lumen.

FS2 ($i = 2$): Basolateral gluten. This subsystem describes the dynamics of gluten peptides that have translocated across the epithelial barrier and are present in the lamina propria at

the basolateral side, where they are available for processing and presentation by antigen-presenting cells. Again, we neglect internal activity and describe this FS by the scalar density

$$f_2 = f_2(t; \hat{u}_2).$$

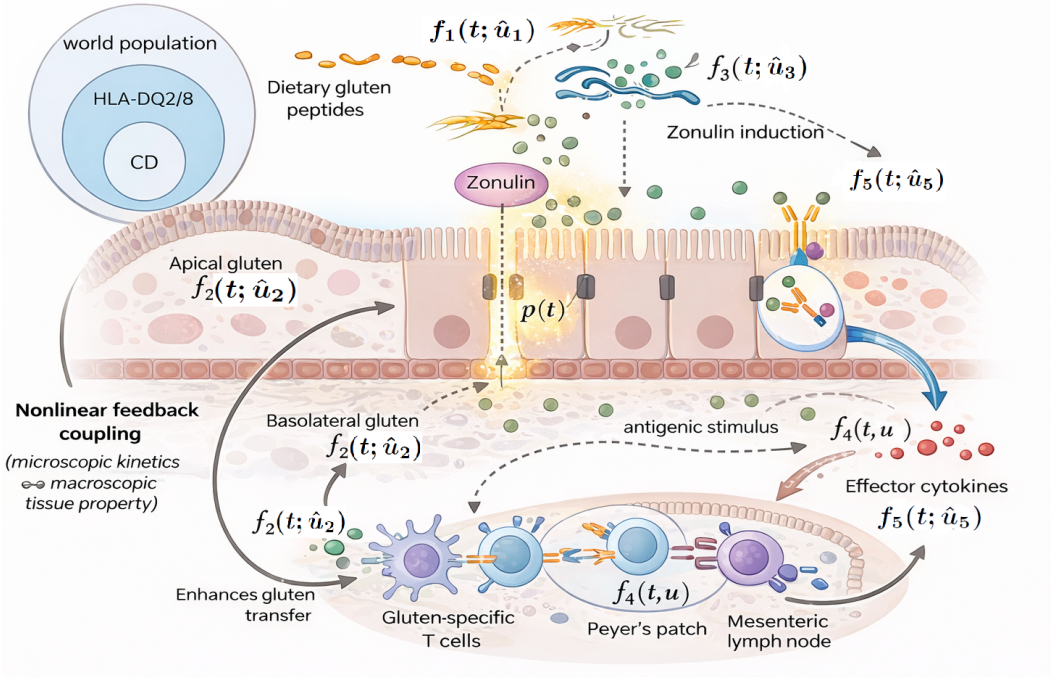

Figure 2. Schematic representation of the multiscale interactions encoded in the KTAP model for coeliac disease. Dietary gluten peptides initiate a cascade involving apical and basolateral transport (f_1, f_2), zonulin release and permeability modulation (f_3, $p(t)$), activation of gluten-specific T-cells (f_4), and secretion of effector cytokines (f_5). The model couples these processes across molecular, cellular, and tissue scales through nonlinear feedback mechanisms, capturing the amplification of immune responses characteristic of the coeliac condition.

FS3 ($i = 3$): Zonulin and permeability-related messengers. This subsystem represents the dynamics of zonulin and related molecular mediators that regulate tight junctions and, consequently, intestinal permeability. These molecules are released in response to apical gluten exposure and modulate the macroscopic variable representing epithelial barrier integrity. Their state is described by

$$f_3 = f_3(t; \hat{u}_3).$$

FS4 ($i = 4$): Gluten-specific T-cells. This subsystem aggregates gluten-specific CD4$^+$ T-cells, including naive, activated, and memory phenotypes. The activation status of each cell is encoded in a microscopic activity variable

$$u \in [0, 1],$$

where $u = 0$ denotes naive or non-activated cells and $u = 1$ corresponds to highly activated or memory effector cells. The state of FS4 is given by the distribution

$$f_4 = f_4(t, u), \qquad u \in D_u = [0, 1].$$

The total T-cell population is

$$n_4(t) = \int_0^1 f_4(t, u)\, du.$$

FS5 ($i = 5$): Effector cytokines. This subsystem represents a lumped population of pro-inflammatory cytokines produced by gluten-specific T-cells, such as TNF, IFN-γ, and related mediators. These molecules contribute to tissue damage and increased permeability. They are modelled by the scalar density

$$f_5 = f_5(t; \hat{u}_5).$$

Macroscopic tissue variable: Intestinal permeability. In addition to the above FSs, we introduce a macroscopic variable

$$p = p(t) \in \mathbb{R}_+,$$

representing the permeability of the small intestine. Low values of p correspond to a tight barrier with intact villi, while high values describe increased permeability and disrupted tight junctions.

Remark 1. *The multiscale character of the model arises not only from the coexistence of entities acting at different biological scales—gluten peptides (molecular scale), cytokines and zonulin (molecular mediators), T-cells (cellular scale), and intestinal permeability (tissue/organ scale)—but also from the hierarchical coupling between these scales. In particular, lower-scale molecular processes regulate higher-scale cellular and tissue-level dynamics, while cross-scale feedback mechanisms further interconnect the system.*

2.2. Model Equations

The model dynamics result from phenomenological assumptions inspired by the biological mechanisms of coeliac disease. We denote by $I(t)$ the exogenous input of gluten into the lumen, corresponding to dietary intake. For simplicity, we assume that the activity variable is fixed for FSs 1, 2, 3, and 5, so that $f_i = f_i(t; \hat{u}_i)$ for $i = 1, 2, 3, 5$. The only FS with an internal activity structure is FS4 (T-cells).

Apical gluten (FS1)

The temporal evolution of apical gluten is governed by dietary intake, degradation, and transfer to the basolateral side through the intestinal barrier:

$$\partial_t f_1(t; \hat{u}_1) = I(t) - d_1 f_1(t; \hat{u}_1) - \Phi\big(p(t)\big)\, f_1(t; \hat{u}_1), \tag{2}$$

where $d_1 > 0$ is the effective degradation or clearance rate of gluten in the lumen, and $\Phi(p)$ is the transfer rate across the epithelial layer.

Basolateral gluten (FS2)

Basolateral gluten increases by translocation from the lumen and decreases by degradation and clearance in the lamina propria:

$$\partial_t f_2(t; \hat{u}_2) = \Phi\big(p(t)\big)\, f_1(t; \hat{u}_1) - d_2 f_2(t; \hat{u}_2), \tag{3}$$

where $d_2 > 0$ is the effective decay rate of basolateral gluten.

Zonulin and permeability messengers (FS3)

Zonulin and related permeability-modulating messengers are produced in response to apical gluten and play a key role in regulating intestinal permeability [23]:

$$\partial_t f_3(t; \hat{u}_3) = c\, f_1(t; \hat{u}_1) - d_3 f_3(t; \hat{u}_3), \tag{4}$$

where $c > 0$ is the rate at which apical gluten induces zonulin production and $d_3 > 0$ is the zonulin decay rate.

Gluten-specific T-cells (FS4)

The distribution $f_4(t,u)$ of gluten-specific T-cells evolves due to activation by basolateral gluten and natural death. Following the KTAP structure used in Equation (1), we write:

$$\begin{aligned}\partial_t f_4(t,u) = f_2(t;\hat{u}_2)\int_0^1 \mu_{42}(u_*)\,\mathcal{B}_{42}(u_* \to u \mid u_*)\,f_4(t,u_*)\,du_* \\ - \mu_{42}(u)\,f_4(t,u)\,f_2(t;\hat{u}_2) - d_4\,f_4(t,u) + \kappa(u) f_2(t;\hat{u}_2) f_4(t,u),\end{aligned} \tag{5}$$

for $u \in [0,1]$, where

- $\mu_{42}(u)$ is the interaction (activation) rate between T-cells of activity u and basolateral gluten. To encode genetic predisposition (e.g., presence of HLA-DQ2/8), we can choose
$$\mu_{42}(u) = \hat{\mu}_{42}(1+u), \qquad \hat{\mu}_{42} \geq 0,$$
with higher values in coeliac subjects compared to tolerant individuals.
- $\mathcal{B}_{42}(u_* \to u \mid u_*)$ is the transition probability density for activity changes upon interaction with antigen. A natural choice is a kernel biased towards higher activation, such that interactions tend to move cells towards larger values of u, as will be specified in the following section. More precisely, the kernel $\mathcal{B}_{42}$ is assumed to satisfy the following standard KTAP properties: (i) non-negativity, $\mathcal{B}_{42}(u_* \to u \mid u_*) \geq 0$; (ii) normalisation,
$$\int_0^1 \mathcal{B}_{42}(u_* \to u \mid u_*)\,du = 1 \quad \text{for all } u_* \in [0,1],$$
which ensures that it defines a probability density; and (iii) activation bias, in the sense that the expected post-interaction activity is larger than or equal to the pre-interaction one.
Under these assumptions, the gain and loss terms in Equation (5) preserve the total number of T-cells in the absence of proliferation and death. Indeed, integrating over $u \in [0,1]$, the contribution of the interaction operator vanishes due to the normalisation of $\mathcal{B}_{42}$, consistently with the conservative structure of KTAP interactions.
- $d_4 > 0$ is the relaxation rate of T-cells.
- $\kappa(u)$ is the proliferation rate of immune cells, which depends on the activation status. The term proportional to $\kappa(u)$ models the clonal expansion of T-cells induced by antigenic stimulation. From a biological viewpoint, activated $CD4^+$ T-cells undergo proliferation upon recognition of antigen-presenting cells, with higher proliferation rates associated with higher activation states [24,25]. This is consistent with the structure of the term, which is proportional to both f_2 (antigen presence) and f_4 (available T-cells). Accordingly, $\kappa(u)$ is taken as an increasing function of u, which is consistent with previous multiscale kinetic models of immune dynamics [18,19].

Effector cytokines (FS5)

Effector cytokines are produced by activated T-cells and decay naturally. Their total density, following the ideas in [19], is modelled as:

$$\partial_t f_5(t;\hat{u}_5) = \int_0^1 r_5(u)\,f_4(t,u)\,du - d_5 f_5(t;\hat{u}_5), \tag{6}$$

where

- $r_5(u)$ is the production rate of effector cytokines by T-cells of activation u. A natural choice is an increasing function of u, for instance

$$r_5(u) = \hat{r}_5(1+u),$$

where $\hat{r}_5$ is the production rate of messengers by the immune system.

Intestinal permeability

The macroscopic permeability $p(t)$ is driven by zonulin and by inflammatory damage mediated by effector cytokines, while relaxing towards lower values in the absence of stimuli. T-cell activity contributes indirectly through cytokine production:

$$p'(t) = \alpha_3 \frac{f_3(t;\hat{u}_3)}{a_3 + f_3(t;\hat{u}_3)} + \alpha_5 \frac{\left(f_5(t;\hat{u}_5) - f_5^{\text{phys}}\right)_+}{a_5 + \left(f_5(t;\hat{u}_5) - f_5^{\text{phys}}\right)_+} - d_p\, p(t), \tag{7}$$

where

- $\alpha_3 > 0$ and $a_3 > 0$ control the effect of zonulin on permeability through a saturating response;
- $\alpha_5 > 0$, $a_5 > 0$ and $f_5^{\text{phys}} \geq 0$ describe the additional damage induced by effector cytokines above a physiological level;
- $d_p > 0$ is the relaxation rate of the epithelial barrier;
- the notation $(\cdot)_+ := \max\{\cdot, 0\}$.

The permeability equation is introduced as an effective phenomenological closure describing the macroscopic response of the epithelial barrier to molecular and cellular stimuli. This formulation is consistent with previous ODE models of coeliac disease, in particular, the one proposed in [26], where permeability is driven by zonulin and inflammatory mediators.

The first term represents zonulin-induced modulation of tight junctions and is modelled through a saturating Hill-type function, reflecting receptor-mediated mechanisms and the limited opening of intercellular junctions. The second term accounts for cytokine-induced tissue damage and is activated only above physiological baseline levels, consistently with the fact that inflammatory effects arise when cytokine concentrations exceed homeostatic thresholds. Both contributions are assumed to saturate for large values of the stimuli, preventing unbounded growth and reflecting biological constraints. The relaxation term models the natural recovery of epithelial integrity in the absence of inflammation.

We stress that this equation is not derived from first principles, but provides a macroscopic closure capturing the aggregate effect of multiple biological mechanisms regulating intestinal permeability.

Summary of the model

Collecting Equations (2)–(6), the KTAP model for coeliac disease is given by the following integro-differential system:

$$
\begin{cases}
\partial_t f_1(t;\hat{u}_1) = I(t) - d_1 f_1(t;\hat{u}_1) - \Phi\big(p(t)\big)\, f_1(t;\hat{u}_1), \\
\partial_t f_2(t;\hat{u}_2) = \Phi\big(p(t)\big)\, f_1(t;\hat{u}_1) - d_2 f_2(t;\hat{u}_2), \\
\partial_t f_3(t;\hat{u}_3) = c\, f_1(t;\hat{u}_1) - d_3 f_3(t;\hat{u}_3), \\
\partial_t f_4(t,u) = f_2(t;\hat{u}_2) \displaystyle\int_0^1 \mu_{42}(u_*)\, \mathcal{B}_{42}(u_* \to u \mid u_*)\, f_4(t,u_*)\, du_* \\
\qquad\qquad -\mu_{42}(u)\, f_4(t,u)\, f_2(t;\hat{u}_2) - d_4\, f_4(t,u) + \kappa(u) f_2(t;\hat{u}_2) f_4(t,u), \\
\partial_t f_5(t;\hat{u}_5) = \displaystyle\int_0^1 r_5(u)\, f_4(t,u)\, du - d_5 f_5(t;\hat{u}_5), \\
p'(t) = \alpha_3 \dfrac{f_3(t;\hat{u}_3)}{a_3 + f_3(t;\hat{u}_3)} + \alpha_5 \dfrac{\big(f_5(t;\hat{u}_5) - f_5^{\mathrm{phys}}\big)_+}{a_5 + \big(f_5(t;\hat{u}_5) - f_5^{\mathrm{phys}}\big)_+} - d_p\, p(t).
\end{cases}
\tag{8}
$$

Remark 2. *The above system reduces, under suitable aggregations and parameter choices, to ODE models similar to those proposed in [26]. The present formulation, however, explicitly accounts for heterogeneity in T-cell activation and for the multiscale interactions between gluten peptides, molecular messengers, immune cells, and tissue-level permeability.*

2.3. Biological Role of Intestinal Permeability

A key feature of coeliac disease is the dysregulation of intestinal permeability, as documented in clinical and translational studies on intestinal barrier function in coeliac patients [2]. Under physiological conditions, the epithelial barrier acts as a selective filter: nutrients are absorbed, whereas large dietary proteins, including immunogenic gluten peptides, remain confined to the intestinal lumen. This selectivity is maintained by tight junctions between epithelial cells, whose opening and closing are tightly regulated.

When permeability increases, this filtering function is compromised. As a consequence, partially digested gluten peptides—particularly the highly immunogenic 33-mer fragments—gain access to the lamina propria. Once in this compartment, gluten peptides are deamidated by tissue transglutaminase (tTG) and presented by HLA-DQ2/8 molecules on antigen-presenting cells. This process triggers the activation and clonal expansion of gluten-specific $CD4^+$ T-cells, which in turn produce pro-inflammatory cytokines such as TNF, IFN-γ, and IL-21. These cytokines damage the epithelium, disrupt tight junctions, and further increase permeability.

Thus, increased permeability is not merely a consequence of inflammation; it is a *driver* of the pathogenic loop. It enables gluten to reach immune-competent regions, amplifies T-cell activation, and sustains a self-reinforcing cycle of inflammation and tissue damage. This positive feedback is central to the chronicity of coeliac disease and to the transition from a healthy to a pathological state.

2.4. Choice of the Transfer Function $\Phi(p)$

Consistent with the ODE model in [26], we assume that transfer is negligible if the permeability is below a critical threshold, and saturates for large permeability, following a Hill-type scheme:

$$
\Phi(p) = \alpha_p \frac{(p - P_{\mathrm{crit}})_+}{a_p + (p - P_{\mathrm{crit}})_+},
$$

where $\alpha_p > 0$ is the maximum transfer rate, $P_{\mathrm{crit}} > 0$ is a critical permeability level, and $a_p > 0$ is a half-saturation constant.

Notice that this structure reflects three biological principles, namely: (i) the existence of a permeability threshold; (ii) a nonlinear increase once the barrier is compromised; and (iii) saturation at high permeability.

Together, these properties ensure that $\Phi(p)$ captures the essential qualitative behaviour of gluten translocation: negligible at low permeability, rapidly increasing once the barrier is compromised and saturating at high permeability. This structure is consistent with previous ODE models of coeliac disease, such as the one proposed in [26], while naturally integrating into the multiscale KTAP framework.

2.5. Analytical Properties of the KTAP System

In this subsection, we establish basic analytical properties of the integro-differential system governing the functional subsystems f_i and the macroscopic permeability variable $p(t)$. These results ensure well-posedness of the model and justify the qualitative behaviour observed in the simulations presented in Section 3.

The mathematical structure of system (8) fits into the general framework of KTAP models developed in previous works on multicellular systems and immune competition [27,28]. In these references, existence, uniqueness, and positivity of mild solutions are established for a broad class of nonlinear kinetic equations with gain–loss operators, bilinear interaction terms, and bounded transition kernels. In the following, we outline how system (8) satisfies the structural assumptions required in these theorems.

The state of the system at each time t is given by

$$U(t) = \big(f_1(t), f_2(t), f_3(t), f_5(t), f_4(t,\cdot), p(t)\big) \in X := \mathbb{R}^4 \times L^1(0,1) \times \mathbb{R}.$$

Solutions are trajectories $U(\cdot) \in C([0,T]; X)$, i.e., continuous in time with values in X. The choice of $L^1(0,1)$ for the T-cell distribution is standard in KTAP models, since $f_4(t,\cdot)$ represents a density over the activity variable and the interaction operators are continuous in L^1.

Now, notice that each equation in (8) is composed of (i) linear decay terms with bounded coefficients; (ii) bounded production terms (e.g., gluten input, zonulin release, cytokine secretion); (iii) bilinear interaction terms of the form $f_i f_j$ with bounded kernels; (iv) integral operators with normalised transition probability densities; and (v) a macroscopic ODE for $p(t)$ with smooth saturating nonlinearities. All coefficients and kernels are assumed to be non-negative and bounded, and the functions $\Phi(p)$, $\mu_{42}(u)$, $\kappa(u)$, and $r_5(u)$ are continuous and bounded on their domains. Under these assumptions, the right-hand side of (8) defines a locally Lipschitz operator on X, as required in the general KTAP theory.

Relying on fixed-point arguments in Banach spaces and on the positivity-preserving structure of KTAP operators, we obtain the following:

Theorem 1 (Well-posedness of the KTAP–CD system)**.** *Let the initial data satisfy $f_i(0) \geq 0$ and $p(0) \in [0, p_{\max}]$. Assume that all coefficients and kernels in system (8) are bounded and non-negative, and that the transition kernel $\mathcal{B}_{42}$ is a probability density. Then there exists a time $T > 0$ and a unique mild solution*

$$U \in C([0,T]; X)$$

to system (8). Moreover, positivity and boundedness are preserved:

$$f_i(t) \geq 0, \qquad p(t) \in [0, p_{\max}], \qquad \forall\, t \in [0,T].$$

For a complete proof, we refer the readers to Refs. [27,28]. We emphasise that the structure of (8) is a direct instance of the general class of nonlinear kinetic equations treated there, and the presence of the macroscopic permeability variable $p(t)$ does not alter the

fixed-point argument, since its evolution is governed by a Lipschitz ODE coupled to the kinetic system.

3. Numerical Results

The mathematical model introduced in Section 2 describes the multiscale interactions between gluten peptides, epithelial permeability, and the adaptive immune response through the integro-differential system (8). To assess the qualitative behaviour of the model and explore its predictive capabilities, we perform a series of numerical simulations that examine how gluten translocation, zonulin release, T-cell activation, and cytokine production jointly shape the intestinal response. Particular attention is paid to the parameters that govern the coupling between functional subsystems, such as the gluten clearance rate, the sensitivity of T-cells to antigenic stimulation, and the impact of zonulin and cytokines on epithelial permeability.

Regarding the activity variable, which is heterogeneously distributed among immune cells from FS4, it will be discretised for computational purposes. We introduce a finite set of discrete activity levels u_j, $j = 1, \ldots, m$, where $u_1 = 0$ and $u_m = 1$ represent the lowest and highest activation states, respectively, while intermediate values correspond to biologically meaningful stages of T-cell responsiveness. The state of the system is therefore described by the discrete probability distribution $\{f_4(t, u_j)\}_{j=1}^{m}$.

In this discrete setting, the transition probability density $\mathcal{B}_{42}$ is replaced by a nearest-neighbour transition kernel. A cell at level u_j may transition to the adjacent higher state u_{j+1} with probability β_1, or to the adjacent lower state u_{j-1} with probability β_2, while remaining at the same level with the complementary probability $1 - \beta_1 - \beta_2$.

This discrete transition operator can be interpreted as a consistent approximation of the continuous kernel $\mathcal{B}_{42}$. In particular, it preserves the key structural properties of the continuous formulation, including non-negativity and normalisation, and ensures conservation of the total T-cell density. Moreover, the bias toward higher activation levels is retained through the choice of transition probabilities, guaranteeing coherence between the continuous model and its numerical implementation.

This simplified structure preserves the directional bias of activation dynamics, ensures mass conservation, and provides a computationally efficient approximation of the continuous transition operator. In addition, following the ideas in [18,19], the proliferation rate of immune cells is modelled as $\kappa(u) = \hat{\kappa}(1 + u)$.

The numerical integration of the discretised system was carried out in MATLAB (R2023b) using the adaptive Runge–Kutta solver `ode45`, which implements the Dormand–Prince method. After discretising the activity variable into $m = 4$ levels, the integro-differential model reduces to a finite-dimensional system of ODEs, which is passed to the routine `ode45` together with the initial condition vector. The integral term in the equation for f_4 is evaluated as a weighted sum over the discrete activity levels. Convergence was verified by repeating simulations with stricter tolerances and with finer activity discretisations, yielding negligible differences in all output variables.

In this section, we focus on two representative case studies corresponding to (i) different physiological conditions and (ii) single and multiple ingestion of gluten.

The initial conditions are listed in Table 1. In addition, Table 2 shows the estimated values of the model parameters and the ranges over which they vary. All reference parameters are taken from previous studies [18,19,26,29]. It is important to comment on the biological grounding of the model parameters. Those directly associated with gliadin dynamics, zonulin release, and epithelial permeability are based on the detailed calibration performed in [26], where the gliadin–zonulin subsystem was fitted to the experimental measurements presented in [30]. In that study, zonulin concentrations were recorded at several time points

after exposing rat intestinal epithelial cells to 0.1 mg/mL of gliadin, and the corresponding model parameters were estimated by minimising the discrepancy between the model output and the experimental data. These fitted values provide biologically grounded estimates for the core components of the coeliac pathway. Parameters for which no coeliac-specific measurements are available were taken from related modelling studies in immunology and epithelial transport, and their ranges were chosen to remain within physiologically plausible regimes.

Table 1. Initial conditions ($t = 0$) for numerical simulations.

Description	Units	Baseline Value
Apical gluten density $n_1(0)$ [26]	mg/mL	0.1
Basolateral gluten density $n_2(0)$ [26]	mg/mL	0.01
Zonulin/permeability messengers $n_3(0)$ [26]	pg/mL	0
T-cell density $n_4(0)$ [26]	cells/mm^3	0.2
Effector cytokines $n_5(0)$ [19]	molecules/mm^3	0
Intestinal permeability $p(0)$ [26]	dimensionless	0.01

Table 2. Summary of model parameters.

Parameter	Meaning	Units	Baseline Value or Range
d_1	Degradation rate of apical gluten (FS1) [26]	1/time	$[0.0324, 0.0363]$
d_2	Decay rate of basolateral gluten (FS2) [26]	1/time	0.001
c	Zonulin production rate induced by apical gluten (FS3) [26]	pg/mL·time	$[0.8638, 0.9065]$
d_3	Zonulin decay rate (FS3) [26]	1/time	$[0.3, 0.7315]$
$\hat{\mu}_{42}$	Baseline activation coefficient [19]	1/time	$[0.001, 0.1]$
d_4	Natural relaxation rate of T-cells (FS4) [29]	1/time	$[0.001, 0.1]$
$\hat{r}_5$	Baseline cytokine production coefficient [19]	1/time	$[0.0001, 0.005]$
d_5	Decay rate of effector cytokines (FS5) [19]	1/time	0.01
α_3	Zonulin-induced permeability increase coefficient [26]	1/time	0.1
a_3	Saturation constant for zonulin effect [26]	pg/mL	3
α_5	Cytokine-induced permeability increase coefficient [26]	1/time	$[0.02, 0.08]$
a_5	Saturation constant for cytokine effect [26]	cells/mm^3	5
f_5^{phys}	Physiological baseline level of effector cytokines	molecules/mm^3	0.01
d_p	Relaxation rate of epithelial barrier permeability [26]	1/time	$[0.008, 0.015]$
P_{crit}	Critical permeability level [26]	dimensionless	$[0.1, 0.15]$
α_p	Maximum transfer rate of gluten from apical to basolateral zone [26]	1/time	$[1, 10]$
a_p	Saturation constant for permeability [26]	dimensionless	$[0.5, 5]$
β_1	Transition towards high activated immune levels [19]	dimensionless	0.1
β_2	Transition towards less activated immune levels [19]	dimensionless	0.05
$\hat{\kappa}$	Proliferation rate of immune cells	mL/time	$[0.1, 1]$

3.1. Single Gluten Challenge

We first examine the response to a single gluten intake. A single ingestion of gluten by someone with coeliac disease or severe sensitivity can trigger acute symptoms like diarrhoea, abdominal pain, and fatigue, typically beginning within an hour and lasting up to several days [31]. This experiment highlights the contrast between a non-coeliac individual, in whom gluten elicits only a mild and self-limited reaction, and a coeliac individual, in whom the same stimulus triggers a markedly amplified immune cascade.

Parameter values and initial conditions are those presented in Tables 1 and 2. Those parameters which are varied for coeliac and non-coeliac individuals are summarised in Table 3.

Table 3. Parameter values used in the non-coeliac and coeliac simulations.

Parameter	Meaning	Non-Coeliac Individual	Coeliac Individual
c	Zonulin production rate induced by apical gluten (FS3)	0.86	0.90
d_3	Zonulin decay rate (FS3)	0.73	0.30
d_4	Natural relaxation rate of T-cells (FS4)	0.03	0.01
α_5	Cytokine-induced permeability coefficient	0.02	0.08
d_p	Permeability relaxation rate	0.012	0.008

In the non-coeliac case, apical gluten is rapidly cleared and only a small fraction crosses the epithelial barrier, resulting in a modest and transient increase in basolateral gluten (panels (a) and (b) of Figure 3). Zonulin release remains limited (panel (c)), permeability exhibits only a slight deviation from baseline (panel (f)), and cytokine levels remain close to physiological values (panel (e)), allowing the system to return quickly to equilibrium.

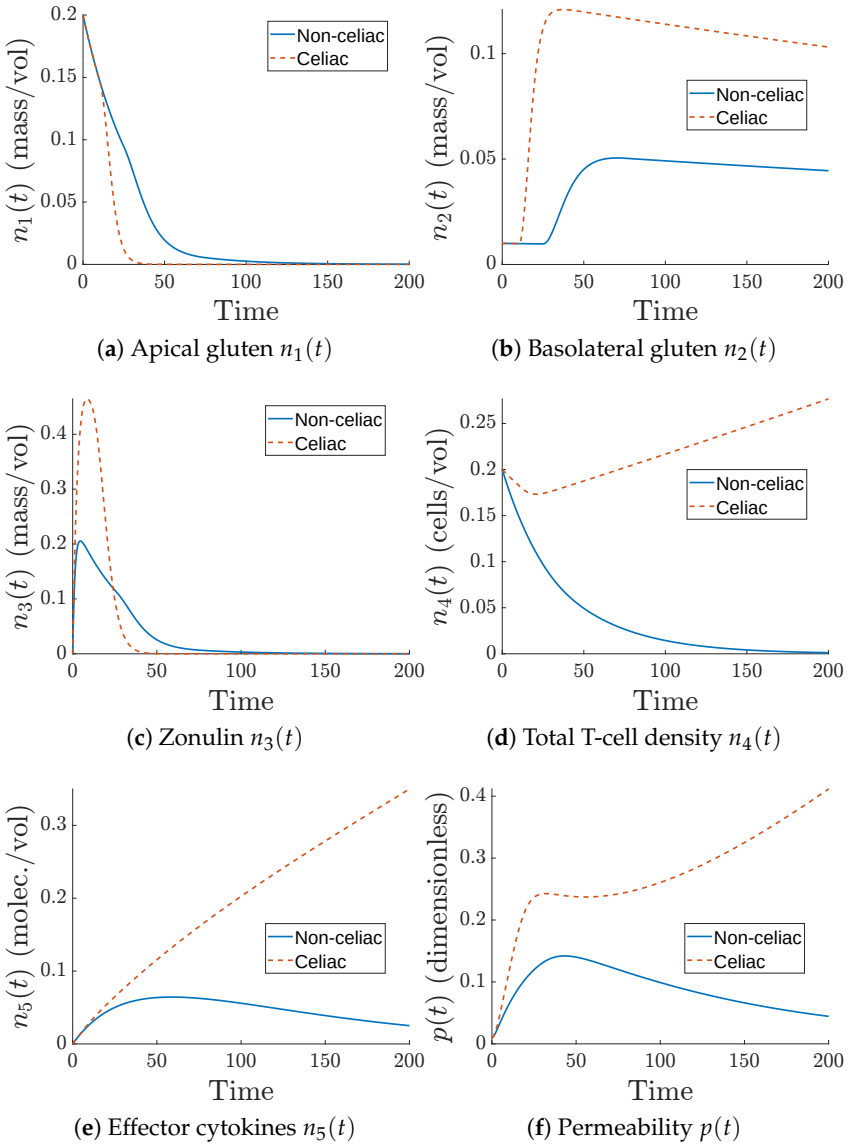

(**a**) Apical gluten $n_1(t)$ (**b**) Basolateral gluten $n_2(t)$

(**c**) Zonulin $n_3(t)$ (**d**) Total T-cell density $n_4(t)$

(**e**) Effector cytokines $n_5(t)$ (**f**) Permeability $p(t)$

Figure 3. Comparison between non-coeliac and coeliac individuals under a single gluten challenge across all functional subsystems. Panels (**a**–**f**) show, respectively: apical gluten $n_1(t)$, basolateral gluten $n_2(t)$, zonulin $n_3(t)$, total T-cell density $n_4(t)$, effector cytokines $n_5(t)$, and epithelial permeability $p(t)$.

In contrast, the coeliac simulation displays a qualitatively different behaviour. The same gluten input produces a larger and more persistent peak in basolateral gluten, which in turn drives a stronger zonulin response and a noticeable increase in permeability. T-cell activation is substantially amplified, leading to a pronounced cytokine burst and a longer-lasting inflammatory episode.

Figure 3 summarises these differences across all functional subsystems.

3.2. Repeated Gluten Exposure

We next examine the effect of periodic gluten intake, mimicking a regular diet.

Gluten intake is modelled as an exogenous forcing term $I(t)$ acting on the apical compartment (FS1). Mathematically, this is implemented through a Bateman-type profile, consisting of a rapid increase followed by an exponential decay, a structure commonly used to describe absorption–elimination processes in pharmacokinetics. This formulation captures the fact that gluten concentration increases abruptly after ingestion but is subsequently cleared by luminal degradation and transit. For repeated dietary exposure, the same pulse is applied periodically, generating a train of Bateman-like inputs that reproduce the oscillatory pattern of gluten appearance associated with regular meals.

In the non-coeliac case, each gluten pulse induces only a small oscillation in apical and basolateral gluten (panels (a) and (b) of Figure 4) and a mild, transient activation of T-cells (panel (d)). Zonulin release remains limited (panel (c)), permeability stays close to baseline (panel (f)), and cytokine levels remain low (panel (e)). The system recovers rapidly between pulses, preventing any cumulative effect.

The coeliac case exhibits a markedly different pattern. Repeated gluten exposure leads to progressive accumulation of basolateral gluten (panel (b)) and sustained activation of T-cells (panel (d)). Zonulin release becomes more pronounced, particularly during the initial pulses (panel (c)), driving a gradual elevation of permeability (panel (f)). Cytokine production increases with each pulse (panel (e)), eventually establishing a chronic inflammatory state. This behaviour reflects the characteristic loss of tolerance observed in coeliac disease.

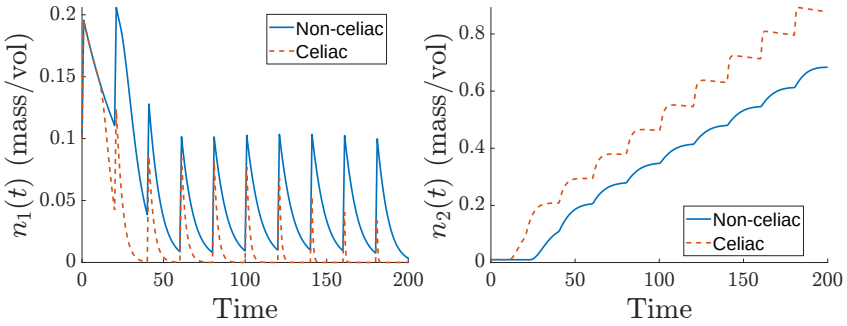

(**a**) Apical gluten $n_1(t)$

(**b**) Basolateral gluten $n_2(t)$

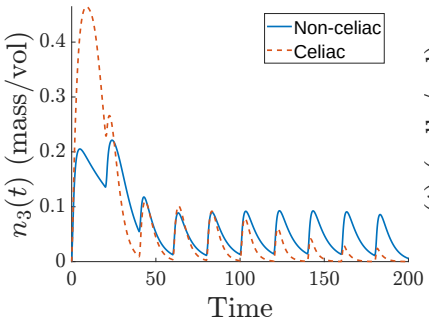

(**c**) Zonulin $n_3(t)$

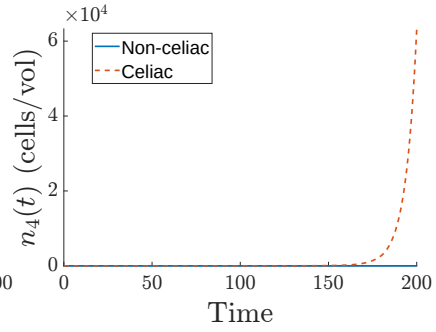

(**d**) Total T-cell density $n_4(t)$

Figure 4. *Cont.*

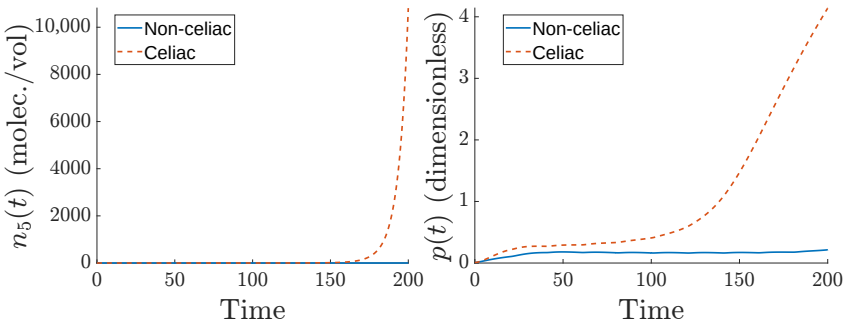

(**e**) Effector cytokines $n_5(t)$ (**f**) Permeability $p(t)$

Figure 4. Comparison between non-coeliac and coeliac individuals under repeated gluten intake across all functional subsystems. Panels (**a**–**f**) show, respectively: apical gluten $n_1(t)$, basolateral gluten $n_2(t)$, zonulin $n_3(t)$, total T-cell density $n_4(t)$, effector cytokines $n_5(t)$, and epithelial permeability $p(t)$.

Figure 4 summarises these differences across all functional subsystems under repeated gluten intake.

3.3. Role of the Proliferation Parameter $\hat{\kappa}$

Finally, we investigate the influence of the proliferation coefficient $\hat{\kappa}$, which modulates the expansion of activated T-cells. This parameter plays a central role in determining whether the immune response remains controlled or becomes pathological.

In the non-coeliac case, increasing $\hat{\kappa}$ from 0.1 to 0.5 produces only moderate changes: cytokine levels rise slightly, but permeability remains stable and the system preserves its ability to return to baseline, as shown in Figure 5. The immune response remains self-limited across the entire range.

In the coeliac case, however, the effect of $\hat{\kappa}$ is dramatic. For $\hat{\kappa} = 0.1$, the response resembles the single-challenge scenario, with a pronounced but transient cytokine peak. As $\hat{\kappa}$ increases to 0.3 and 0.5, the system undergoes a qualitative transition: T-cell activation becomes self-sustaining, cytokine levels grow explosively, and permeability rises sharply, as can be seen in Figure 6. This behaviour reveals a bifurcation structure in which $\hat{\kappa}$ acts as a control parameter separating a stable regime from a pathological inflammatory state.

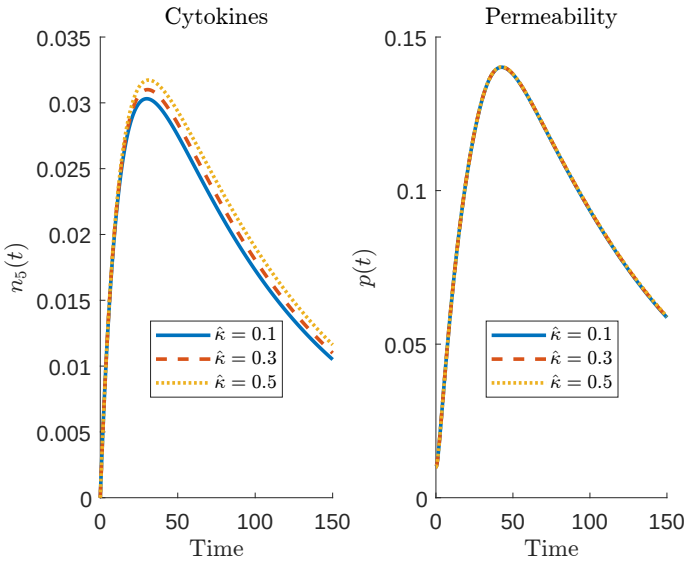

Figure 5. Cytokines and permeability under varying $\hat{\kappa}$ in the non-coeliac case.

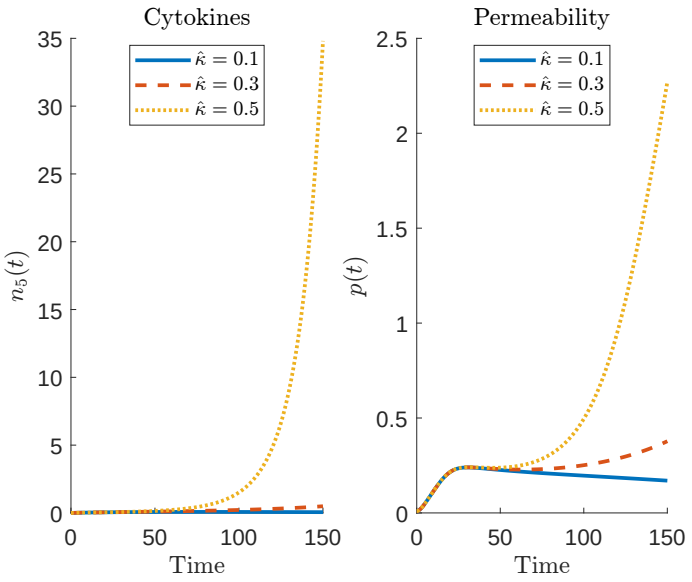

Figure 6. Cytokines and permeability under varying $\hat{\kappa}$ in the coeliac case.

4. Conclusions and Perspectives

This work has introduced a multiscale mathematical model for coeliac disease based on the kinetic theory of active particles. The model integrates the dynamics of gluten peptides, zonulin-mediated modulation of intestinal permeability, and the activation of gluten-specific T-cells and effector cytokines. The resulting framework captures the multiscale nature of the system through entities acting at different biological scales, from molecular messengers to cellular populations and tissue-level responses. This multiscale structure constitutes the main novelty of the present contribution, as it allows for the emergence of pathological patterns from the interplay of processes that cannot be understood in isolation.

The concept of messenger plays a central role in this setting. Zonulin, cytokines, and permeability-related signals act as sub-particle entities that mediate the interactions between active particles, shaping the transition from gluten ingestion to epithelial damage. The model formalises how these messengers orchestrate the coupling between gluten dynamics (FS1 and FS2), immune activation (FS4), and epithelial responses, while incorporating feedback loops that sustain inflammation in genetically predisposed individuals. Our model captures the nonlinear feedback loops that drive the transition from a healthy state to chronic inflammation in genetically susceptible individuals. Numerical simulations reproduce key qualitative features of coeliac disease, including transient immune activation in non-coeliac individuals and amplified, persistent responses in the coeliac condition. These results highlight the potential of multiscale kinetic models to explain the nonlinear mechanisms underlying autoimmune disorders.

A critical analysis of the model suggests several directions for further mathematical development. The present formulation points toward the derivation of more general differential systems capable of describing multicellular and molecular interactions with higher resolution. This includes the possibility of incorporating additional sub-particle scales, such as intracellular signalling pathways or gene-level regulatory mechanisms, which are increasingly recognised as essential in the immunopathology of coeliac disease. These perspectives are consistent with recent developments in the kinetic theory of active particles [16,17,32], where multiscale interactions are regarded as a natural extension of the theory. Indeed, all these considerations motivate the further development of the kinetic theory of active particles toward a fully multiscale framework, where the interactive dynamics of cells, sub-particles, and molecular mediators can be represented within a unified differential structure.

This research direction is reinforced by recent advances in immunology, including the 2025 Nobel Prize in Medicine, awarded for contributions that operate precisely at the interface between molecular-, cellular-, and tissue-level immune processes [22]. Within such a scientific landscape, the KTAP framework offers a natural mathematical setting for modelling the complexity of autoimmune diseases, complementing previous applications to infectious diseases [33] and cancer dynamics [28].

In addition to these mathematical perspectives, the model also offers biologically meaningful insights into the mechanisms underlying coeliac disease. By formalising the coupling between gluten translocation, zonulin-mediated permeability changes, and T-cell activation, the model connects naturally with existing immunological frameworks that emphasise HLA-DQ2/8-restricted antigen presentation, cytokine-driven amplification loops, and barrier dysfunction as central drivers of pathology. At the same time, several limitations must be acknowledged. Innate immune components and spatial heterogeneity are represented in a simplified manner, parameter estimates rely partly on semi-quantitative evidence, and the model is not intended to provide quantitative clinical predictions. Nevertheless, the structure of the model highlights potential therapeutic leverage points—such as interventions targeting epithelial permeability or modulating gluten processing—that align with current biological understanding and motivate future refinements.

Beyond mathematical considerations, the model opens avenues for dialogue with biomedical and clinical research. By providing a structured representation of the mechanisms that drive disease onset and progression, it may contribute to the design of predictive tools capable of exploring patient-specific scenarios, dietary exposures, or therapeutic interventions. Such tools could support the development of personalised strategies for disease management, bridging the gap between theoretical modelling and clinical practice.

In summary, this work advances the mathematical study of coeliac disease by formalising the multiscale interactions that underlie its immunopathology. The model's structure and simulations illustrate the potential of kinetic approaches to capture the nonlinear dynamics of autoimmune responses. Further refinement and empirical validation will be essential steps toward transforming these theoretical insights into practical contributions for biomedical research and clinical applications.

Author Contributions: Conceptualization, D.B., D.A.K. and L.S.; Methodology, D.B., D.A.K. and L.S.; Software, D.A.K.; Validation, D.B. and L.S.; Formal analysis, D.B., D.A.K. and L.S.; Investigation, D.B., D.A.K. and L.S.; Resources, D.B., D.A.K. and L.S.; Writing—original draft, D.B., D.A.K. and L.S.; Writing—review and editing, D.B., D.A.K. and L.S.; Visualization, D.B., D.A.K. and L.S.; Funding acquisition, D.A.K. All authors have read and agreed to the published version of the manuscript.

Funding: Damian A. Knopoff acknowledges the support by Grant PID2023-146872OB-I00-DyCMaMod funded by MICIU/AEI/10.13039.501100011033 and by Feder, EU.

Data Availability Statement: The original contributions presented in this study are included in the article. Further inquiries can be directed to the corresponding author.

Conflicts of Interest: The authors declare that they have no known competing financial interests or personal relationships that could have appeared to influence the work reported in this paper.

References

1. Husby, S.; Koletzko, S.; Korponay-Szabó, I.R.; Mearin, M.L.; Phillips, A.; Shamir, R.; Troncone, R.; Giersiepen, K.; Branski, D.; Catassi, C.; et al. European Society for Pediatric Gastroenterology, Hepatology, and Nutrition Guidelines for the Diagnosis of Coeliac Disease. *J. Pediatr. Gastroenterol. Nutr.* **2012**, *54*, 136–160. [CrossRef]
2. Martínez Velasco, S. Permeabilidad Intestinal en Pacientes Celíacos. Ph.D. Thesis, Universidad del País Vasco UPV-EHU, Bilbao, Spain, 2025.

3. Caio, G.; Volta, U.; Sapone, A.; Leffler, D.A.; De Giorgio, R.; Catassi, C.; Fasano, A. Celiac Disease: A Comprehensive Current Review. *BMC Med.* **2019**, *17*, 142. [CrossRef]
4. Fasano, A.; Catassi, C. Celiac Disease. *N. Engl. J. Med.* **2012**, *367*, 2419–2426. [CrossRef]
5. Singh, P.; Arora, A.; Strand, T. A.; Leffler, D. A.; Catassi, C.; Green, P. H.; et al. Global Prevalence of Celiac Disease: Systematic Review and Meta-Analysis. *Clin. Gastroenterol. Hepatol.* **2018**, *16*, 823–836. [CrossRef] [PubMed]
6. Serrano, L.; Rodriguez-Herrera, A.; Serrat, C.; Rubio-Escudero, C. Introducing Joint Modeling Techniques for Personalized Predictions in Celiac Disease. *Gastroenterology* **2022**, *162*, S361–S362. [CrossRef]
7. van de Wal, Y.; Kooy, Y.; van Veelen, P.; Peña, S.; Mearin, L.; Papadopoulos, G.; Koning, F. Cutting edge: Selective Deamidation by Tissue Transglutaminase Strongly Enhances Gliadin-Specific T Cell Reactivity. *J. Immunol.* **1998**, *161*, 1585–1588. [CrossRef]
8. Sollid, L.M. The Roles of MHC Class II Genes and Post-Translational Modification in Celiac Disease. *Immunogenetics* **2017**, *69*, 605–616. [CrossRef]
9. Pagliari, D.; Urgesi, R.; Frosali, S.; Riccioni, M.E.; Newton, E.E.; Lolfi, R.; Polfi, F.; Cianci, R. The Interaction among Microbiota, Immunity, and Genetic and Dietary Factors Is the Condicio Sine Qua Non Celiac Disease Can Develop. *J. Immunol. Res.* **2015**, *2015*, 123653. [CrossRef] [PubMed]
10. Abadie, V.; Kim, S.M.; Lejeune, T.; Palanski, B.A.; Ernest, J.D.; Tastet, O.; Voisine, J.; Discepolo, V.; Marietta, E.V.; Hawash, M.B.; et al. IL-15, Gluten and HLA-DQ8 Drive Tissue Destruction in Coeliac Disease. *Nature* **2020**, *578*, 600–604. [CrossRef] [PubMed]
11. Meresse, B.; Curran, S.A.; Ciszewski, C.; Orbelyan, G.; Setty, M.; Bhagat, G.; Lee, L.; Tretiakova, M.; Semrad, C.; Kistner, E.; et al. Reprogramming of CTLs into Natural Killer–Like Cells in Celiac Disease. *J. Exp. Med.* **2006**, *203*, 1343–1355. [CrossRef]
12. Boersma, B.; Wynne, H.; Wit, J. A Mathematical Model Describing Catch-Up Growth in Celiac Disease. *Acta Paediatr.* **1994**, *83*, 1097–1099. [CrossRef] [PubMed]
13. Schumann, M.; Siegmund, B.; Schulzke, J.D.; Fromm, M. Celiac Disease: Role of the Epithelial Barrier. *Cell. Mol. Gastroenterol. Hepatol.* **2017**, *3*, 150–162. [CrossRef]
14. Abadie, V.; Sollid, L.M.; Barreiro, L.B.; Jabri, B. Integration of Genetic and Immunological Insights into a Model of Celiac Disease Pathogenesis. *Annu. Rev. Immunol.* **2011**, *29*, 493–525. [CrossRef]
15. Hamam, H. Mathematical Modeling of Immune-Mediated Villi Damage in Celiac Disease: Th1/Th2 Dynamics Under Gluten Exposure and Withdrawal. *Int. J. Biomath.* **2025**, *18*, 5501153. [CrossRef]
16. Bellomo, N.; Burini, D.; Dosi, G.; Gibelli, L.; Knopoff, D.A.; Outada, N.; Terna, P.; Virgillito, M.E. What Is Life? A Perspective of the Mathematical Kinetic Theory of Active Particles. *Math. Models Methods Appl. Sci.* **2021**, *31*, 1821–1866. [CrossRef]
17. Bellomo, N.; Burini, D.; Liao, J. New Trends in Kinetic Theory toward the Complexity of Living Systems. *Math. Models Methods Appl. Sci.* **2026**, *36*, 341–397. [CrossRef]
18. Bellomo, N.; Eftimie, R.; Forni, G. What Is the In-Host Dynamics of SARS-CoV-2 Virus? A Challenge within a Multiscale Vision of Living Systems. *Netw. Heterog. Media* **2024**, *19*, 655–681. [CrossRef]
19. Burini, D.; Knopoff, D.A. A Multiscale Kinetic Theory Approach to Viral–Immune Competition. *Math. Models Methods Appl. Sci.* **2026**, *36*, 1307–1324. [CrossRef]
20. Commins, S.P.; Borish, L.; Steinke, J.W. Immunologic Messenger Molecules: Cytokines, Interferons, and Chemokines. *J. Allergy Clin. Immunol.* **2010**, *125*, S53–S72. [CrossRef]
21. Melchjorsen, J. Learning from the Messengers: Innate Sensing of Viruses and Cytokine Regulation of Immunity—Clues for Treatments and Vaccines. *Viruses* **2013**, *5*, 470–527. [CrossRef] [PubMed]
22. Nobel Assembly at Karolinska Institutet. Nobel Prize in Physiology or Medicine 2025—Press Release. Available online: https://www.nobelprize.org/uploads/2025/10/press-medicineprize2025.pdf (accessed on 28 February 2026).
23. Dafonte, T.M.; Valitutti, F.; Kenyon, V.; Locascio, J.J.; Montuori, M.; Francavilla, R.; Passaro, T.; Crocco, M.; Norsa, L.; Piemontese, P.; et al. Zonulin as a Biomarker for the Development of Coeliac Disease. *Pediatrics* **2024**, *153*, e2023063050. [CrossRef]
24. Abbas, A.K.; Lichtman, A.H.; Pillai, S. *Cellular and Molecular Immunology*, 8th ed.; Elsevier: Philadelphia, PA, USA, 2014.
25. Murphy, K.; Weaver, C. *Janeway's Immunobiology*, 9th ed.; Garland Science: New York, NY, USA, 2016.
26. Trask, J.M. Modeling Celiac Disease. Master's Thesis, The University of Tennessee, Knoxville, TN, USA, 2014.
27. Bellouquid, A.; Ch-Chaoui, M. Asymptotic analysis of a nonlinear integro-differential system modeling the immune response. *Comput. Math. Appl.* **2014**, *68*, 905–914. [CrossRef]
28. Bellouquid, A.; Delitala, M. *Modelling Complex Biological Systems—A Kinetic Theory Approach*; Birkhäuser–Springer: Basel, Switzerland, 2006.
29. Bar-On, Y.M.; Flamholz, A.; Phillips, R.; Milo, R. SARS-CoV-2 (COVID-19) by the Numbers. *eLife* **2020**, *9*, e57309. [CrossRef]
30. Clemente, M.G.; De Virgiliis, S.; Kang, J.S.; Macatagney, R.; Musu, M.P.; Di Pierro, M.R.; Drago, S.; Congia, M.; Fasano, A. Early effects of gliadin on enterocyte intracellular signalling involved in intestinal barrier function. *Gut* **2003**, *52*, 218–223. [CrossRef]
31. Silvester, J.A.; Graff, L.A.; Rigaux, L.; Walker, J.R.; Duerksen, D.R. Symptomatic Suspected Gluten Exposure Is Common among Patients with Coeliac Disease on a Gluten-Free Diet. *Aliment. Pharmacol. Ther.* **2016**, *44*, 612–619. [CrossRef]

32. Bellomo, N.; Egidi, M. From Herbert A. Sims Legacy to the Evolutionary Artificial World with Heterogeneous Collective Behaviors. *Math. Models Methods Appl. Sci.* **2024**, *34*, 145–180. [CrossRef]
33. Bertaglia, G.; Bondesan, A.; Burini, D.; Eftimie, R.; Pareschi, L.; Toscani, G. New Trends on the Systems Approach to Modeling SARS-CoV-2 Pandemics in a Globally Connected Planet. *Math. Models Methods Appl. Sci.* **2024**, *34*, 1995–2054. [CrossRef]